Exploring single-molecule SERS and single-nanoparticle plasmon microscopy

Kristin L. Wustholz[a], Anne-Isabelle Henry[a], Julia M. Bingham[a], Samuel L. Kleinman[a], Michael J. Natan[b], R. Griffith Freeman[b], Richard P. Van Duyne*[a]
[a]Northwestern University, Department of Chemistry, 2145 Sheridan Rd., Evanston, IL 60201
[b]Oxonica Materials, Inc., 325 E. Middlefield Rd., Mountain View, CA 94043, USA

ABSTRACT

In this work we perform correlated structural and optical studies of single nanoparticles as well as explore the generality of SMSERS. First, wide-field plasmon resonance microscopy is used to simultaneously determine the LSPR spectra of multiple Ag nanoprisms, whose structure is determined using TEM. Next, the structure-property relationships for well-defined and easily-controlled nanoparticle structures (e.g. monomers, dimers, and trimers) are studied using correlated TEM, LSPR, and SERS measurements of individual SERS nanotags. We present the SER spectrum of reporter molecules on a single nanotag comprised of a Au trimer. It was determined that of 40 individual nanotags, just 19 exhibited SERS. The remaining nanoparticles were established by TEM to be monomers. These results demonstrate that SERS signal is observed from individual nanotags containing a junction or hot spot. Lastly, we explore crystal violet, a triphenyl methane dye that was used in the seminal SMSERS investigations, and re-examine single-molecule sensitivity using the isotopologue approach.

Keywords: Localized surface plasmon resonance, surface-enhanced Raman spectroscopy, crystal violet, SERS nanotags, nanoprisms, single-nanoparticle spectroscopy, wide-field imaging, LSPR imaging, transmission electron microscopy

INTRODUCTION

Metal nanoparticles exhibit brilliant colors under white-light illumination, a consequence of the localized surface plasmon resonance (LSPR), the phenomenon responsible for the colors in the Roman Lycurgus Cup as well as antique stained glass windows.[1, 2] Scientific interest in metallic particles dates to the 19th century, when Michael Faraday examined size and color relationship of Au particles.[3] It was later determined that excitation of the LSPR of metallic surfaces having nanoscale features results in local electromagnetic field enhancement.[4, 5] Indeed, the Raman scattering intensity of pyridine on electrochemically roughened Ag was observed to be enhanced by ~10^6.[6] This remarkable discovery led to the emergence of surface-enhanced Raman spectroscopy (SERS),[7, 8] a technique that proved to be a powerful tool for fundamental studies of surface adsorbates. Advances in nanofabrication methods that produce substrates with controlled and well-defined plasmonic properties, along with improvements in laser sources, detection schemes, and theoretical modeling provide the basis for our current understanding of SERS. In addition, the discovery of single-molecule SERS (SMSERS) in 1997[9, 10] has generated heightened interest in both the fundamentals of the technique as well as its application to chemical analysis. Although several decades have passed since the discovery of SERS, quite fundamental questions remain unanswered. For example, what nanoparticle structure or array provides the highest electromagnetic enhancement? This question is significant since the development of next generation LSPR- and SERS-based sensors requires the development of the most enhancing nanoparticles and nanoparticle arrays. Therefore, an understanding of the fundamental relationships among the SER scattering intensity, LSPR, and nanoparticle structure must be established.

Toward this end, recent interest has focused on correlated investigations of structure (i.e., with AFM or TEM imaging) and LSPR for individual nanoparticles as well as the corresponding SER spectra for adsorbed analytes, which provide the ability to study the fundamental relationships between the structural and optical properties at the single-particle level, unobscured by ensemble-averaging. For example, triangular Ag nanoprisms[11] exhibit a bulk LSPR spectrum with a maximum (λ_{max}) at ~650 nm.

*vanduyne@chem.northwestern.edu; phone 1 847 491-3516; fax 1 847 491-4530; www.chem.northwestern.edu/~vanduyne

Plasmonics: Metallic Nanostructures and Their Optical Properties VII, edited by Mark I. Stockman,
Proc. of SPIE Vol. 7394, 739403 · © 2009 SPIE · CCC code: 0277-786X/09/$18 · doi: 10.1117/12.826168

However, it was demonstrated using single-nanoparticle spectroscopy that individual Ag nanoprisms have LSPR ranging from at least 600 to 700 nm.[12] Although the Ag nanoprism solution is more monodisperse relative to a citrate-reduced Ag colloid solution, the observation disperse single-nanoparticle LSPR maxima is consistent with the existence of various nanoparticle geometries. Since Ag nanoprisms are similarly shaped with modest structural differences they are an excellent system in which to examine the detailed LSPR-structure correlation. In the first part of this work we demonstrate high-throughput single-nanoparticle spectroscopy correlated to structural characterization by TEM, which enables the rapid characterization of the plasmon and structural distribution of the Ag nanoprisms. In addition, previous work has demonstrated that cube-shaped nanoparticles fabricated using polyol synthesis[13] exhibit two LSPR maxima owing to the asymmetry induced by surface immobilization on glass.[14] Both LSPR peaks are sensitive to changes in dielectric environment, but the blue-shifted resonance has superior LSPR sensing capabilities due to its sharpness.[15] Correlated LSPR and high-resolution TEM measurements of individual Ag nanocubes revealed the dependence of the LSPR on nanocube size and shape.[14] Corresponding electrodynamics calculations demonstrated the strong sensitivity between the nanocube optical response and the face-to-face width, corner and side rounding, and substrate of each nanocube. In a related study, correlated high-resolution scanning electron microscopy and polarization-dependent SERS measurements were performed on individual Ag nanocubes.[16] Although the Ag nanocube samples appeared monodisperse, various SER scattering intensities were observed from individual nanocubes as a result of nanoparticle orientation relative to the exciting laser field. Ensemble-averaged SERS experiments on the nanocubes reveal that the overall average enhancement factor (EF) is $\sim 10^5$ although detailed studies at the single-nanoparticle level are needed to elucidate the underlying details of the electromagnetic enhancement.[17]

Ultimately, the most desirable single-particle experiment is to measure the structure, LSPR, and SER scattering intensity from the *same* nanoparticle. At present, single-molecule SERS (SMSERS) experiments have provided the best example of this correlated study.[18, 19] However, the Ag colloids used in the majority of SMSERS experiments are randomly aggregated using electrolyte solutions and do not provide controlled, homogeneous structures. To avoid the use of aggregated colloidal nanoparticles, novel nanostructures composed of a stabilizing shell around a well-defined metallic core have been developed. For example, SERS nanotags containing Au cores, a layer of a SERS "reporter" molecule, and silica shell have demonstrated structural uniformity, optical robustness, and the capability to use bio-relevant reporter molecules.[20] Moreover, these SERS nanotags provide an excellent system in which to study the structure-property relationships for well-defined nanoparticle structures (e.g. monomers, dimers, trimers).[21] Another major challenge for the widespread application of single-molecule SERS (SMSERS) has been that just a handful of analytes (e.g., rhodamine 6G, nile blue) have demonstrated single-molecule signal. Indeed, it has been recently recognized that several observations commonly used to establish single-molecule detection such as blinking and Poisson-distributed scattering intensities are problematic.[22, 23] Therefore, a significant goal is to establish the generality of SMSERS by exploring various classes of chromophores as well as nonresonant species.

In this work we perform correlated structural and optical studies of single nanoparticles as well as explore the generality of SMSERS. First, wide-field plasmon resonance microscopy is used to simultaneously determine the LSPR spectra of multiple Ag nanoprisms immobilized on TEM grids. The structure of the Ag nanoprisms is then measured using TEM. Next, the structure-property relationships for well-defined and easily-controlled nanoparticle geometries (e.g. monomers, dimers, and trimers) are studied using correlated TEM, LSPR, and SERS measurements of individual SERS nanotags. Lastly, we explore crystal violet, a triphenyl methane dye that was used in one of the seminal SMSERS investigations,[10] and establish single-molecule detection using the isotopologue approach.

2. METHODOLOGY

2.1 Materials

Ag nanoprisms were synthesized according to a previously reported procedure.[11] Briefly, 0.1 mM $AgNO_3$ was stirred in the presence of sodium citrate (0.3 mM) on ice, followed by the addition of cold $NaBH_4$ (1 mL, 50 mM). To aid in the stabilization of the particles, bis(*p*-sulfonatophenyl)-phenylphosphine dihydrate dipotassium (BSPP) (1 mL, 5 mM) was added dropwise. The solution was stirred strongly on ice for 1 h then stirred at a reduced speed for 3-4 h. The resulting yellow solution (composed of spherical Ag nanoparticles) was irradiated for 4-5 h with white light through a 550-nm bandpass filter to yield a green solution comprised of Ag nanoprisms. The Ag nanoprism solution was centrifuged at 10,000 rpm for 5 min and rinsed twice with deionized H_2O (Millipore Milli-Q, 18.2 $M\Omega \bullet cm^{-1}$). Next, 30 μL of solution

was drop cast on a TEM grid (Ted Pella, 300 mesh) on filter paper in 10 μL increments and allowed to dry. SERS nanotags comprised of aggregated 90-nm diameter Au spheres coated with a reporter, 2-(4-Pyridyl)-2-cyano-1-(4-ethynylphenyl)ethylene, and then 20-nm SiO_2 were used as received (Oxonica Inc). The particles were deposited on a TEM grid (Ted Pella, 200 mesh) by drop casting a 10-μL aqueous solution. Crystal violet (CV-d_0) and deuterated crystal violet (CV-d_{12}) were used as received from Sigma-Aldrich and the Scheidt group at Northwestern University, respectively. Silver colloids were synthesized according to the Lee and Miesel procedure.[24] Briefly, 90 mg of $AgNO_3$ in 500 mL of deionized water was brought to a rapid boil with stirring. While boiling, 10 mL of a 1% sodium citrate (Sigma-Aldrich) solution was added. The initially clear solution turned transparent yellow and then an opaque gray-green in 30 mins, after which it was cooled to room temperature and diluted to 420 mL with water. SMSERS samples were prepared by mixing 100 μL of 50:50 mixture of CV-d_0 (5×10^{-10} M) to CV-d_{12} (5×10^{-10} M) with a 1-mL aliquot of Ag colloids (~10^{-9} M) such that on average, 1 dye molecule is adsorbed per nanoparticle. The dye-colloid solution was then diluted with 1 mL of 20 mM NaCl solution to induce nanoparticle aggregation. A 10 μL sample of the resulting solution was drop cast on piranha-etched, base-treated glass coverslip and allowed to dry. The coverslip was then mounted in a custom designed flow cell and immersed in a dry N_2 environment. Ag island films (AgIFs) were fabricated by electron beam evaporation (Kurt J. Lesker Co., AXXIS) of 6 nm Ag (Kurt J. Lesker Co., 99.999%) at a rate of 1 Å•s^{-1} onto piranha-etched, base-treated glass coverslips (Fisher). The AgIFs were incubated in aqueous solutions of CV for 4-6 h.

2.2 Transmission electron microscopy

TEM measurements were performed on copper TEM grids coated with a 50-nm thick film of formwar and a 2-3 nm thick layer of amorphous carbon (Ted Pella, 200-300 mesh). Transmission electron micrographs were obtained on a JEOL JEM-2100F Fast TEM operating at 200kV.

2.3 Localized surface plasmon resonance spectroscopy

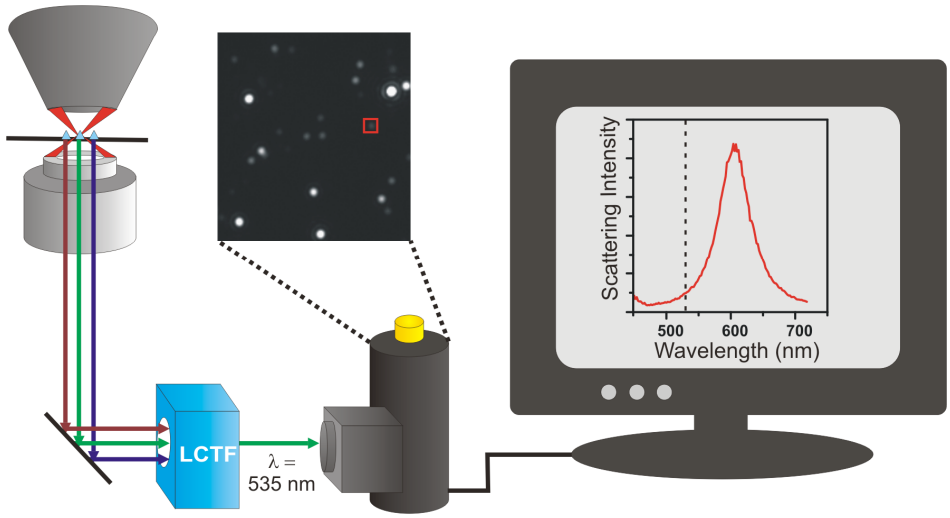

Fig. 1. Schematic of the wide-field LSPR imaging and spectroscopy experimental setup. Images of the resonant Rayleigh scattering intensity are collected at a particular wavelength through a LCTF onto a CCD detector. Here, the scattering intensity image at 535 nm is shown. By analyzing images using home-built software the LSPR spectra of all imaged particles are simultaneously measured.

The wide-field LSPR imaging and spectroscopy experiments were performed on an inverted microscope (Nikon Eclipse Ti-U) equipped with a dark-field condenser (Nikon, NA = 0.80-0.95) and a variable numerical aperture 100x oil-immersion objective (Nikon, Plan Fluor, 100X, NA = 0.5-1.3, oil, iris) set to NA = 0.5 to collect only the resonant Rayleigh scattered light from the nanoparticles. The experimental setup is depicted in Figure 1. The scattered light from multiple nanoparticles was sent through a liquid crystal tunable filter (LCTF) (CRi VariSpec), which has a continuously tunable transmission from 400 nm to 720 nm with a spectral bandwidth of 7 nm, to a LN_2-cooled CCD detector (Princeton Instruments Spec-10 400B). The LCTF was scanned from 400 nm to 720 nm with 2 nm increments, collecting

a series of wide-field intensity images, where each frame has associated wavelength information. The scattering intensity of each nanoparticle was integrated as a function of wavelength to construct single nanoparticle spectra. All measurements were obtained in ambient atmosphere.

LSPR spectra of individual SERS nanotags were measured on an inverted microscope (Nikon TE300) using white-light illumination through a dry dark-field condenser (Nikon, NA = 0.7-0.95). Scattering from the sample was collected through an oil-immersion objective equipped with a variable numerical aperture (NA) iris set to NA = 0.5 (Nikon, Plan Fluor, 100X, NA = 0.5-1.3, oil, iris) onto a 1/3-m monochromator containing a low-dispersion grating blazed at 500 nm (150 groove•mm^{-1}) and detected by a LN_2-cooled CCD camera (Princeton Instruments, Spec-10 400BR). Individual diffraction-limited spots were centered on the entrance slit of the spectrograph and LSPR spectra were collected from ~400 to 900 nm with typical acquisition times (t_{acq}) of 10 s.

2.4 Surface-enhanced Raman spectroscopy

SERS samples containing crystal violet were illuminated using a diode-pumped solid-state laser operating at 532 nm (Spectra-Physics, Millenia X). Oxonica nanotags were illuminated at 632.8 nm with a HeNe laser (Research Electro-Optics, 17 mW) through a cleanup filter (Semrock, NF03-633E-25). Samples were placed on an inverted microscope (Nikon TE300) equipped with a 100x oil-immersion objective with NA = 0.5 5 (Nikon, Plan Fluor, 100X, NA = 0.5-1.3, oil, iris). The emerging light was filtered (Omega Optical, 540AELP or Semrock, LL01-633-25) analyzed using a 1/3 m imaging spectrograph equipped with a 1200 groove•mm^{-1} grating blazed at 500 nm (Acton 300i), and collected with a LN_2-cooled CCD camera (Princeton Instruments, Spec-10 400B). For ensemble-averaged studies samples were illuminated in the epi-illumination geometry with an excitation power (P_{exc}) of ~ 100W•cm^{-2} and t_{acq} = 5 s. For single-molecule studies, the samples were illuminated at grazing incidence with P_{exc} ~ 2W•cm^{-2} and t_{acq} = 10 s.

3. RESULTS

3.1 Correlated wide-field LSPR and TEM measurements of individual Ag nanoprisms

The LSPR of single Ag nanoparticles was measured using a modified wide-field resonant Rayleigh scattering spectroscopy method.[25] In this configuration, the resonant Rayleigh scattered light of isolated particles deposited on a TEM grid is imaged and the diffraction-limited spots are pattern matched to the particles in a TEM image. A LCTF was added to the experimental setup in order to precisely select the wavelength of the scattered light that is collected by the detector. As a result, LSPR data from of tens of particles is acquired at one wavelength per acquisition instead of recording the LSPR spectrum of just one particle. Therefore, the wide-field LSPR imaging method collects multiple single-nanoparticle spectra in parallel, increasing the throughput and efficiency of single-nanoparticle spectroscopy.

Silver nanoparticles composed primarily of nanoprisms were synthesized and investigated using correlated TEM measurements and wide-field LSPR imaging. These largely monodisperse samples, which have demonstrated modest variability among individual nanoparticles, provide an interesting system to characterize the impact of minute structural changes on the optical properties at the single-nanoparticle level. Figures 2a and 2b presents images of scattering intensity in the same region of interest at wavelengths corresponding to 535 nm and 640 nm, respectively. In these images white areas are diffraction-limited spots corresponding to mainly single particles and occasionally aggregates of two to three particles. The image size (i.e., 20.1 μm ±0.5 μm x 51.4 μm ±0.5 μm) corresponds to the actual region of spectral data acquisition, almost half of a 300-mesh TEM square. Figures 2a and 2b demonstrate disperse relative scattering intensities of the Ag nanoprisms, consistent with a distribution of individual nanoparticle structures. Moreover, some of the particles exhibit high scattering intensity at 535 nm but not at 640 nm, and vice versa.

Two particles of interest are highlighted in Figures 2a and 2b, designated as particle 1 and particle 2. The corresponding scattering spectra of these particles are shown in Figures 2c and 2d. The spectra are obtained by plotting the scattering intensity of the particle as a function of wavelength in the experimental range. To illustrate this point, two lines (blue and red) have been drawn on the spectra of particles 1 and 2 at 535 nm and 640 nm. The scattering intensity of particle 2 at 535 nm is much lower relative to particle 1. Moreover, particle 1 exhibits two LSPR peaks with λ_{max} at 564 nm and 641 nm, whereas the spectrum of particle 2 contains one peak, with λ_{max} corresponding to 629 nm. The difference in the number of peaks and the position of the LSPR is

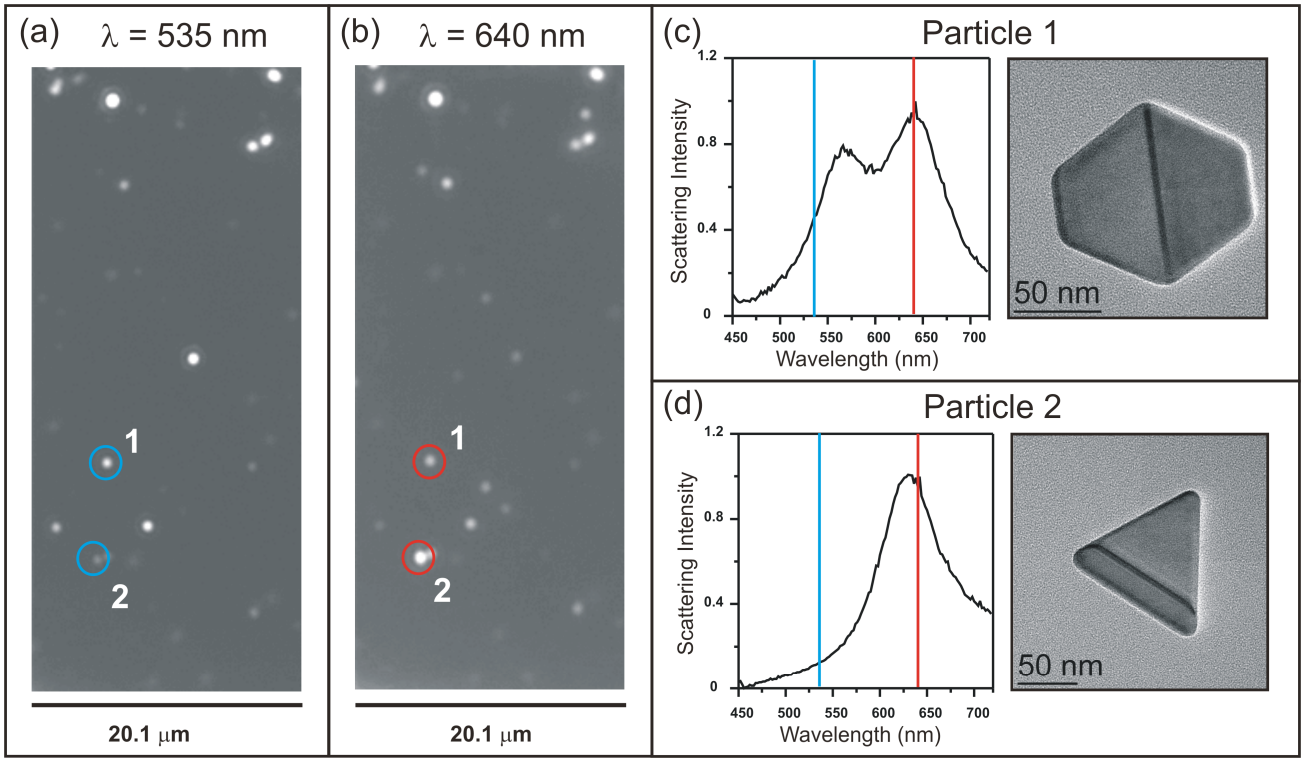

Fig. 2. Wide-field resonant Rayleigh scattering images of multiple Ag nanoparticles on a TEM grid at 535 nm (a) and 640 nm (b). Corresponding scattering spectra (left) and TEM images (right) of the highlighted particles 1 and 2 are presented in (c) and (d), respectively.

consistent with differences in particle structure. In particular, it has been demonstrated that the truncature, size, and shape influence both the position and number of LSPR peaks.[26] The structures of particles 1 and 2 were determined by TEM, as shown on the right of the spectra in Figures 2c and 2d. Particle 2 corresponds to an equilateral triangle of 100 nm in edge length. Particle 1 is a hexagonal particle that may be the result of the fusion of two truncated triangles, consistent with the observation of inhomogeneous contrast on both particles, which reveals defects in crystallinity. These structural observations are consistent with the measured LSPR spectra. Ultimately, these results demonstrate the capabilities of the wide-field LSPR imaging and spectroscopy method, which provide the ability to image tens to hundreds of diffraction-limited spots and determine their LSPR spectra in a field approximately half the size of a TEM square.

3.2 Correlated LSPR, TEM, and SERS measurements of individual nanotags

The optical and structural properties of indivdual SERS nanotags were determined using correlated TEM, LSPR, and SERS measurements of immobilized particles on a TEM grid. Figure 3a presents the transmission electron micrograph of a SERS nanotag, which consists of three Au cores coated in the SERS reporter and encapsulated by a silica shell. The LSPR of the nanoparticle is presented in Figure 3b, demonstrating two resonant Rayleigh scattering maxima at approximately 640 nm and 815 nm. The existence of more than one LSPR maximum is consistent with the aggregated structure of the nanotag.

Figures 3c and 3d exhibit SER spectra of nanotags following laser excitation at 632.8 nm, which are consistent with the normal Raman spectrum of the reporter molecule (not presented). The ensemble-averaged SER spectrum (Figure 3d) was obtained by measuring a cluster of nanotags immobilized on a TEM grid. The SER spectrum in Figure 3c corresponds to signal from reporter molecules on the nanotag trimer pictured in Figure 3a and exhibits high intensity (i.e., ~10^5 counts mW^{-1} s^{-1} for the Raman band at 1600 cm^{-1}). Moreover, of 40 individual nanotags, just 19 exhibited SERS. The remaining nanoparticles were determined by TEM to be monomers. Therefore, SERS signal from an individual nanotag is possible if it contains a hot spot, consistent with predictions of the electromagnetic enhancement mechanism.[27] In order to

determine the impact of nanoparticle structure on electromagnetic properties of specific nanostructures and SERS enhancements, additional correlated TEM, LSPR, and SERS measurements are underway.

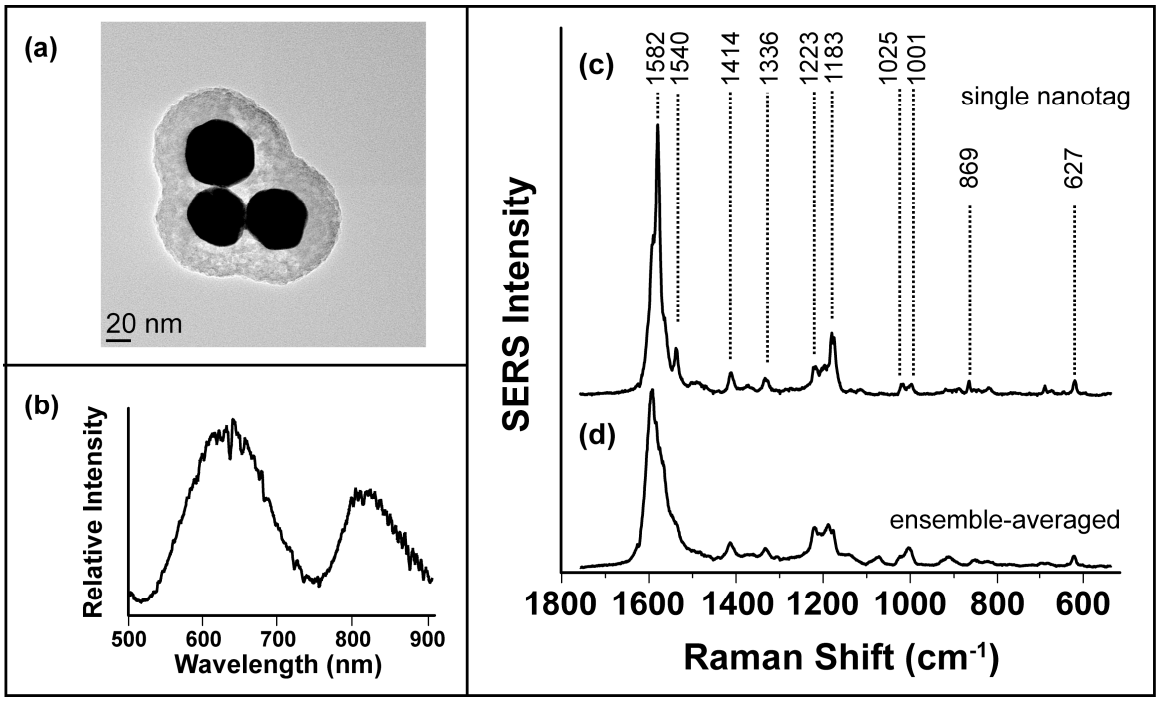

Fig. 3. Correlated TEM (a), resonant Rayleigh scattering (b), and SERS from an individual nanotag (c). The SER spectrum from the single nanotag is consistent with the ensemble-averaged spectrum obtained from a cluster of nanotags immobilized on a TEM grid (d).

3.3 SMSERS of crystal violet isotopologues

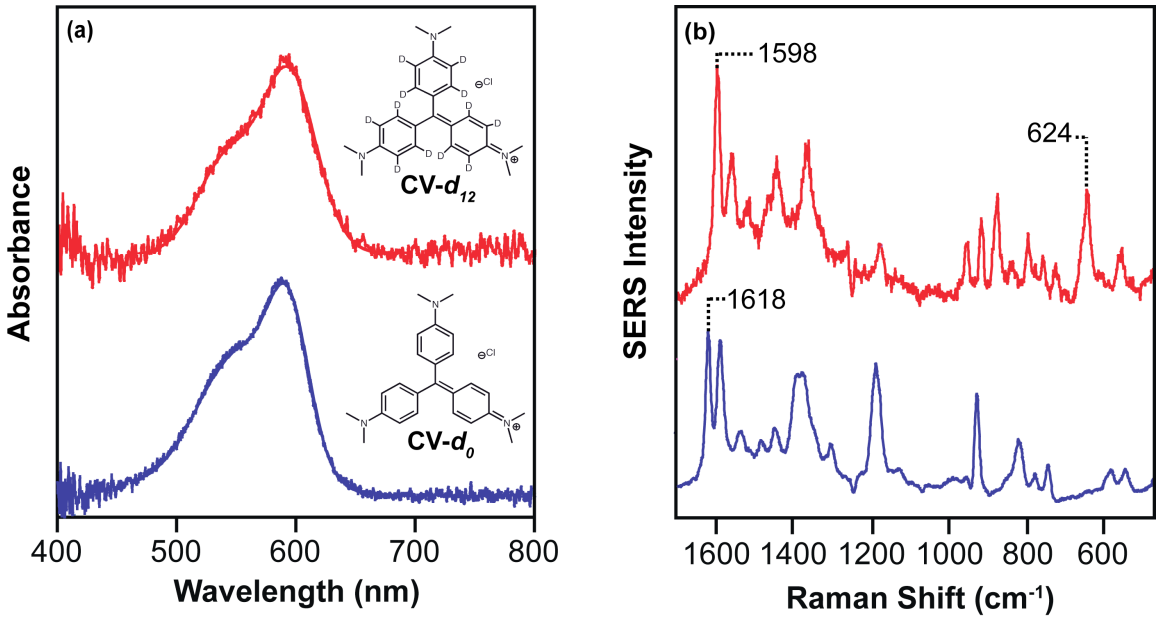

Fig. 4. Characterization of crystal violet (CV) isotopologues: (a) Absorbance spectra of CV-d_0 (blue) and CV-d_{12} (red) with λ_{max} = 590 nm, and (b) SER spectra of CV-d_0 (blue) and CV-d_{12} (red) obtained on AgIFs with λ_{exc} = 532 nm, P_{exc} < 2 mW, t_{acq} = 5s. Characteristic vibrational bands of the isotopologues are highlighted.

The ensemble-averaged optical properties of the CV isotopologues are summarized in Figure 4. As expected, the molecular absorbance of undeuterated and deuterated CV (Figure 4a) are identical in lineshape and extinction maximum (i.e., λ_{max} = 590 nm). Bulk SERS measurements were performed by incubating AgIFs in dye solutions and illuminating the rinsed, dried substrates with 532 nm laser excitation. The ensemble-averaged SER spectrum of CV-d_0 measured shows prominent peaks at 917, 1175, and 1618 cm^{-1} in agreement with prior reports.[28, 29] The ensemble-averaged SER spectrum of CV-d_{12} is similar to that of its protonated analog, in agreement with previous measurements, [27] but contains distinguishable peaks. For example, the Raman bands at >1600 cm^{-1} for the protonated species are shifted to <1600 cm^{-1}.[30] Additionally, CV-d_{12} exhibits a strong Raman band at 624 cm^{-1} that is not present in the protonated molecule, consistent with previous work.[29] Ultimately, Figure 4b demonstrates the essence of the isotopically-edited bi-analyte approach; the isotopologues are structurally and electronically similar and yet spectrally distinguishable with SERS. For this experiment the presence or absence of the spectral features at >1600 cm^{-1} and 624 cm^{-1} was used to establish the identity of the chromophore on the SMSERS nanoparticle aggregates.

SMSERS measurements of crystal violet were performed on Ag colloids using the isotopologue approach.[19] In this method the target analyte molecule (CV-d_0) is mixed in equimolar quantity with its vibrationally distinct isotopologue (CV-d_{12}) in low concentrations with a solution of aggregated Ag colloids. It has been established that the junctions between nanoparticles support hot spots where extremely intense electromagnetic fields are concentrated. The enhanced fields experienced by molecules in hot spots provide greatly enhanced Raman signal, allowing for single-molecule detection.[27] In the isotopologue approach, the detection of single molecules is verified by performing measurements on many nanoparticle aggregates to ensure statistical significance, that is, either one or other isotopologue is most commonly observed.[19, 31-33]

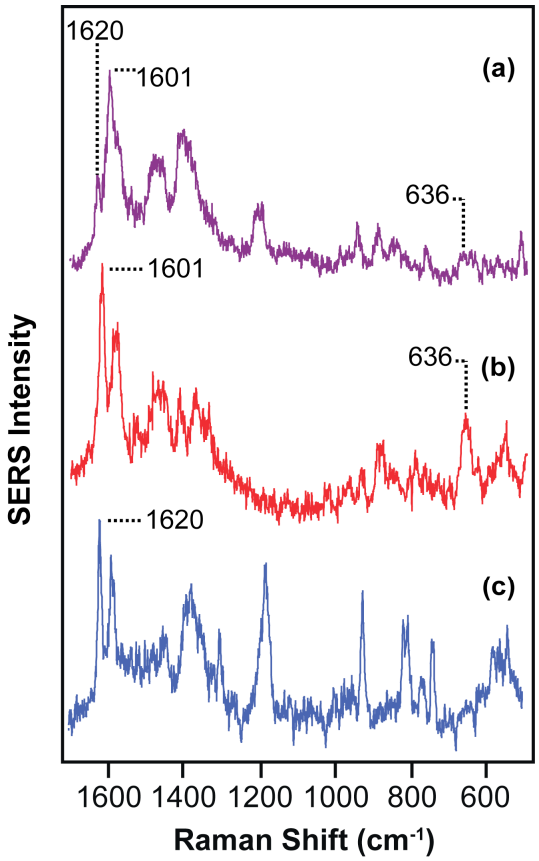

Fig. 5. Representative SMSER spectra of CV isotopologues: (a) both CV-d_0 and CV-d_{12} (purple), (b) only CV-d_{12} (red), and (c) only CV-d_0 (blue) obtained using λ_{max} = 532 nm, P_{exc} ~20 mW, t_{acq} 10 s.

Figure 5 presents representative SER spectra obtained under single-molecule conditions (i.e., aggregated Ag colloids immobilized on glass containing ~1 molecule per nanoparticle). Spectral features from both CV-d_0 *and* CV-d_{12} are evident in the spectrum presented in Figure 5a, an observation consistent with both molecules existing in the hot spot. In contrast, the SMSER spectra in Figures 5b and 5c are identified as originating from *either* CV-d_0 *or* CV-d_{12}. These preliminary results demonstrate that the isotopologue approach can be used to establish single-molecule sensitivity for a triphenyl methane chromophore. The results presented herein are the first isotopically-edited SMSERS experiment conducted on any member of the triphenyl methane family of dyes. To date approximately 15 SMSER spectra of CV have been obtained, but to ensure statistical significance ~100 total spectra will be obtained and analyzed; such work is underway. Ultimately, by exploring several resonant chromophores as well as nonresonant species, we hope to expand the generality and utility of SMSERS.

CONCLUSIONS

Recent interest has focused on correlated investigations of structure and LSPR for individual nanoparticles as well as the corresponding SER spectra for adsorbed analytes. Such detailed studies provide the ability to study the fundamental relationships between structural and optical properties at the single-particle level, unobscured by ensemble-averaging. In this work we explored the structural and optical studies of single nanoparticles and aggregates as well as explore the generality of SMSERS. First, wide-field LSPR imaging and spectroscopy were used to simultaneously determine the LSPR spectra of multiple Ag nanoprisms immobilized on TEM grids. These measurements demonstrated that wide-field LSPR spectroscopy removes the need to isolate each particle in the field of view, thereby increasing the efficiency of single-nanoparticle spectroscopy. We expect that the high-throughput wide-field LSPR imaging method which employs a LCTF will be important to enhance our understanding of the effect of minute nanoparticle structural changes on the LSPR. Next, SER signal was obtained from reporter molecules on a single nanotag comprised of a Au trimer with ~10^5 counts mW^{-1} s^{-1} for the Raman band at 1600 cm^{-1}. Of 40 individual nanotags investigated, just 19 exhibited SERS, where the remaining nanoparticles were established by TEM to be monomers. Lastly, we explored SMSERS of crystal violet using the isotopologue approach. We anticipate that such studies performed at the single-molecule and single-nanoparticle levels will greatly enhance our understanding of the operative structure-property relationships in plasmonic substrates as well as provide the means to optimize next-generation LSPR- and SERS-based sensors.

ACKNOWLEDGEMENTS

We thank Eric Phillips and Prof. Karl Scheidt at Northwestern University for generously providing the deuterated crystal violet isotopologue. This research was supported by the NSF (CHE-0414554, CHE-0911145), AFOSR/DARPA Project BAA07-61 (FA9550-08-1-0221), NSF NSEC (EEC-0647560), and NSF MRSEC (DMR-0520513) at the Materials Research Center of Northwestern University. We thank the NU*ANCE* Center at Northwestern University for providing access to the TEM equipment.

REFERENCES

[1] D. J. Barber and I. C. Freestone, "An investigation of the origin of the colour of the Lycurgus Cup by analytical transmission electron microscopy," Archaeometry 32, 33-45 (1990).

[2] R. H. Brill, "The chemistry of the Lycurgus cup," Proceedings of the 7th International Congress on Glass, comptes rendus 2. 1-13 (1965).

[3] M. Faraday, "The Bakerian Lecture: Experimental Relations of Gold (and Other Metals) to Light," Philosophical Transactions of the Royal Society of London 147, 145-181 (1857).

[4] K. A. Willets and R. P. Van Duyne, "Localized surface plasmon resonance spectroscopy and sensing," Annu. Rev. Phys. Chem. 58, 267-297 (2007).

[5] G. C. Schatz, M. A. Young and R. P. Van Duyne, [Electromagnetic mechanism of SERS] Springer-Verlag Berlin, Berlin, (2006).

[6] M. Fleischmann, P. J. Hendra and A. J. McQuillan, "Raman spectra of pyridine adsorbed at a silver electrode," Chem. Phys. Lett. 26, 163-166 (1974).
[7] M. G. Albrecht and J. A. Creighton, "Anomalously intense Raman spectra of pyridine at a silver electrode," J. Am. Chem. Soc. 99, 5215-5217 (1977).
[8] D. L. Jeanmaire and R. P. Van Duyne, "Surface Raman spectroelectrochemistry 1. Heterocyclic, aromatic, and aliphatic-amines adsorbed on anodized silver electrode," J. Electroanal. Chem. 84, 1-20 (1977).
[9] S. Nie and S. R. Emory, "Probing single molecules and single nanoparticles by surface-enhanced Raman scattering," Science (Washington, D. C.) 275, 1102-1106 (1997).
[10] K. Kneipp, Y. Wang, H. Kneipp, L. T. Perelman, I. Itzkan, R. R. Dasari and M. S. Feld, "Single molecule detection using surface-enhanced Raman scattering (SERS)," Physical Review Letters 78, 1667-1670 (1997).
[11] R. Jin, Y. Cao, C. A. Mirkin, K. L. Kelly, G. C. Schatz and J. G. Zheng, "Photoinduced Conversion of Silver Nanospheres to Nanoprisms," Science 294, 1901-1903 (2001).
[12] L. J. Sherry, R. Jin, C. A. Mirkin, G. C. Schatz and R. P. Van Duyne, "Localized Surface Plasmon Resonance Spectroscopy of Single Silver Triangular Nanoprisms," Nano Lett. 6, 2060-2065 (2006).
[13] A. R. Siekkinen, J. M. McLellan, J. Y. Chen and Y. N. Xia, "Rapid synthesis of small silver nanocubes by mediating polyol reduction with a trace amount of sodium sulfide or sodium hydrosulfide," Chem. Phys. Lett. 432, 491-496 (2006).
[14] J. A. McMahon, Y. M. Wang, L. J. Sherry, R. P. Van Duyne, L. D. Marks, S. K. Gray and G. C. Schatz, "Correlating the Structure, Optical Spectra, and Electrodynamics of Single Silver Nanocubes," Journal of Physical Chemistry C 113, 2731-2735 (2009).
[15] L. J. Sherry, S. H. Chang, G. C. Schatz, R. P. Van Duyne, B. J. Wiley and Y. N. Xia, "Localized surface plasmon resonance spectroscopy of single silver nanocubes," Nano Lett. 5, 2034-2038 (2005).
[16] J. M. McLellan, Z. Y. Li, A. R. Siekkinen and Y. N. Xia, "The SERS activity of a supported Ag nanocube strongly depends on its orientation relative to laser polarization," Nano Lett. 7, 1013-1017 (2007).
[17] J. M. McLellan, A. Siekkinen, J. Y. Chen and Y. N. Xia, "Comparison of the surface-enhanced Raman scattering on sharp and truncated silver nanocubes," Chem. Phys. Lett. 427, 122-126 (2006).
[18] J. P. Camden, J. A. Dieringer, J. Zhao and R. P. Van Duyne, "Controlled Plasmonic Nanostructures for Surface-Enhanced Spectroscopy and Sensing," Acc. Chem. Res. 41, 1653-1661 (2008).
[19] J. A. Dieringer, R. B. Lettan, K. A. Scheidt and R. P. Van Duyne, "A frequency domain existence proof of single-molecule surface-enhanced Raman Spectroscopy," J. Am. Chem. Soc. 129, 16249-16256 (2007).
[20] W. E. Doering, M. E. Piotti, M. J. Natan and R. G. Freeman, "SERS as a foundation for nanoscale, optically detected biological labels," Adv. Mater. 19, 3100-3108 (2007).
[21] J. McMahon, A.-I. Henry, K. Wustholz, M. Natan, G. Freeman, R. Van Duyne and G. Schatz, "Gold nanoparticle dimer plasmonics: Finite element method calculations of the electromagnetic enhancement to surface-enhanced Raman spectroscopy," Analytical and Bioanalytical Chemistry ABC-00162-02009 (2009).
[22] P. G. Etchegoin, M. Meyer and E. C. Le Ru, "Statistics of single molecule SERS signals: is there a Poisson distribution of intensities?," Phys. Chem. Chem. Phys. 9, 3006-3010 (2007).
[23] P. C. Andersen, M. L. Jacobson and K. L. Rowlen, "Flashy silver nanoparticles," Journal of Physical Chemistry B 108, 2148-2153 (2004).
[24] P. C. Lee and D. Meisel, "Adsorption and surface-enhanced Raman of dyes on silver and gold sols," J. Phys. Chem. 86, 3391-3395 (1982).
[25] J. J. Mock, M. Barbic, D. R. Smith, D. A. Schultz and S. Schultz, "Shape effects in plasmon resonance of individual colloidal silver nanoparticles," The Journal of Chemical Physics 116, 6755-6759 (2002).
[26] K. L. Kelly, E. Coronado, L. L. Zhao and G. C. Schatz, "The Optical Properties of Metal Nanoparticles: The Influence of Size, Shape, and Dielectric Environment," Journal of Physical Chemistry B 107, 668-677 (2003).
[27] J. P. Camden, J. A. Dieringer, Y. M. Wang, D. J. Masiello, L. D. Marks, G. C. Schatz and R. P. Van Duyne, "Probing the structure of single-molecule surface-enhanced Raman scattering hot spots," J. Am. Chem. Soc. 130, 12616 (2008).
[28] M. V. Canamares, C. Chenal, R. L. Birke and J. R. Lombardi, "DFT, SERS, and Single-Molecule SERS of Crystal Violet," Journal of Physical Chemistry C 112, 20295-20300 (2008).
[29] S. Sunder and H. J. Bernstein, "Resonance Raman Spectrum of a deuterated crystal violet," Can. J. Chem.-Rev. Can. Chim. 59, 964-967 (1981).
[30] J. Gicquel, M. Carles and H. Bodot, "Resonance Raman investigation of charge-transfer complexes between a trityl cation (crystal violet) and sulfonated azo derivatives," J. Phys. Chem. 83, 699-706 (1979).

[31] P. G. Etchegoin, M. Meyer, E. Blackie and E. C. Le Ru, "Statistics of single-molecule surface enhanced Raman scattering signals: Fluctuation analysis with multiple analyte techniques," Anal. Chem. 79, 8411-8415 (2007).
[32] E. Blackie, E. C. Le Ru, M. Meyer, M. Timmer, B. Burkett, P. Northcote and P. G. Etchegoin, "Bi-analyte SERS with isotopically edited dyes," Phys. Chem. Chem. Phys. 10, 4147-4153 (2008).
[33] E. C. Le Ru, M. Meyer and P. G. Etchegoin, "Proof of single-molecule sensitivity in surface enhanced Raman scattering (SERS) by means of a two-analyte technique," Journal of Physical Chemistry B 110, 1944-1948 (2006).